Experimental study of the Performance of a Venturi-Meter with Suspended Gas-Solid Flow

I. M. Sakr[1], W. A. El-Askary[1, 2], Mohamed M. Sheha[1], Tarek A. Ghonim[1]

[1] *Mechanical Power Engineering Department, Faculty of Engineering, Menoufia University, Shebin El-Kom Egypt, 32511*
[2] *Alexandria Higher Institute of Engineering and Technology (AIET), Alexandria, Egypt*
(Corresponding Author Email: Ismailsakr@yahoo.com)

ABSTRACT

Due to the urgent need for electricity sources in Egypt, this investigation is an attempt to prepare a metering tool for measuring the flow rate of the suspended gas-solid mixture flows in coal thermal power stations. One of the simplest methods for accurately measuring the flow rate of pulverized coal in the thermal power stations is the venturi meter. In the present work, different geometrical models have been designed and applied for measuring air-coal mixture flow rate, considering the effect of different operational parameters on the pressure sensitivity, pressure recovery and performance of the venturi models. The measurements showed the effects of these parameters on the pressure drop and the pressure distribution. New charts have been deduced from the experimental data for seven non-standard venturi models that shows different effects of particle size, loading ratio and throat length of venturi. From the experimental results a new correlation for two-phase flow discharge coefficient is deduced in the present study. The comparison between the experimental and correlation has been done with error percentage from +25% to -20%.

Keywords: Gas-solid; Two-Phase flow, Geometrical parameters; Operational parameters.

1. INTRODUCTION

Measuring solids flow rates of the gas-solid flow has been considered and become important in the industrial processes including furnaces, thermal power stations, and pneumatic pipelines. The venturi meter method has been used widely for measuring single-phase flow with a high degree of accuracy because of the small losses occurring through it. However, the main difficulties appear when using a device for measuring two-phase flow such gas-solid flow. Because of its low cost, and simplicity, venturi meter became an important tool for measuring the gas-solid flow in the thermal power stations. During the past and present decades, different researches were interesting for such a field.

Gas- particle mixture. Gas- particle flow is just one of the portion of the flow region referred to as a two-phase flow. The classification of two-phase flow is the combination of any two of the three states of matter; solid, liquid, and gas phase. Two-phase flow can also be classified by the geometry of the interface; that is

separated flows, mixed flows, and dispersed flows. Modeling approaches suitable for design predictions of Andhra Pradesh (AP) have been examined, while numerical models provide a clearer understanding of this phenomenon which occurs in scrubbers. Analytical models offer the most promise for improving industrial design practice [1-2]. There is a significant amount of research into the pressure response of a Venturi meter conveying two-phase flow to measure the flow rate, but the behavior of the flow inside the Venturi has not been thoroughly explored [3]. Numerical simulations of the weaken turbulent gas-solid two-phase flow in a horizontal Venturi tube were used to contemplate the impacts of Venturi tube geometry on the pressure distribution in the mixture [4-5]. The pressure drop due to the flow of the air–coal mixture increases with the increase of superficial air velocity, gas density, and volumetric loading ratio [6-8]. The velocity of the gas-solid mixture in the convergent section increases with

increasing the diameter ratio, while a sharp pressure drop and hence energy loss are noticed [9-10].

Two pressure drop signals were determined to indicate that the flow of the entrained solids is independent of solid to gas ratio when calculating according to an empirically developed equation of the pressure drop across different points of the Venturi [11-13]. Gary and Anthony [14] demonstrated that the two-phase flow depends critically on empirical calibration for any chosen two-phase flow metering system. The effects of solids loading and gas velocity on the pressure drop within the packed bed were investigated by Wang et al. [15]. An innovative capacitive system for the concentration measurement of gas-solid flow in pneumatically conveyed pulverized fuel at power stations has been developed [16]. The performance of Venturi scrubber depends on many factors, some of them are droplet dispersion, pressure drop, atomization, size of droplets, injection method and collection mechanism see Ref. [17]. The experimental results of measuring gas-solid flow in venturi developed a correlation giving a good prediction to the overreading of four nonstandard Venturi meters with a prediction error of ±4% and uncertainty less than ±2.5% [18-19].

Based on the experimental data, a numerical simulation of transport of pulverized fuel in a complex splitting device, has been carried out in [20]. Additionally, the transportation pattern of fly ash gradually changed from sparse–dense flow to partial and plug flows with increasing conveying distance because of the conveying pressure loss [21]. An experimental work had been investigated on a vertical Venturi feeder with the conveying system operating in the dilute-phase regime with 1 mm spherical glass particles. The experimental solids flow rate presented a linear relationship with the airflow rate for the vertical Venturi feeder, due to the decreasing pressure in the throat and no appreciable leakage through the feeding pipe [22]. A proposed model predicted both particle collection and pressure drop applied to the whole Venturi including entrance nozzle, throat, and diffuser [23]. Experiments were conducted with air and solid flow rates representative of the lean pneumatic conveying typically used in power stations to discover whether the technique was specifically suited to this application [24]. The model took into account the momentum, heat, and mass transfer between the continuous phase and the dispersed phase. It was found that the drying rate increases as the inlet gas temperature or the gas mass flow rate increases, while it decreases as the solid mass flow rate is increased [25-26].

Zhang et al. [27] established a two-phase flow model and validated it by comparing pressure prediction with traditional models in oil and gas wells. The main objective of the present research is the preparation of a metering tool (Venturi meter) for suspended gas-solid mixture flows that can be used in coal thermal power stations. The venturi performance and correlations will be deduced from the obtained results based on the metering tool.

2. EXPERIMENTAL TEST RIG

The present experimental test rig is illustrated schematically in Fig. (1) with the necessary equipment's which are used in the research: The primary air flows in an open cycle, in which a screw compressor (1) is used to supply the required motive air steadily, after storing it in an air tank (3), at a maximum pressure of 8 bars. The pressure is controlled by a pressure control valve (4) and a pressure regulator (6). The motive air is delivered to a primary flow convergent-divergent nozzle (7), which is placed along the axis of the ejector (8). Due to the negative pressure at the primary flow nozzle exit, a mixture of secondary air flow suspending solids entrains to the ejector which is controlled by the secondary flow control valve 1 (12) from the main reservoir of pulverized coal (29). The entrained air-solid mixture then enters the mixing convergent duct (9) and straight duct (10). In the mixing duct, both primary air, secondary air, and solid mixture are mixed. The total flow is then discharged to a conical tail diffuser (11) added at the end of the mixing straight duct aiming to increase the static pressure recovery up to the atmospheric pressure, where the flow is exhausted to the tested venturi (13). Orifice (5) and Pitot-tube (24) are respectively installed in the primary air flow passage to evaluate the required measurements. Moreover, pressure taps (17) are installed in the convergent, throat, and divergent sections (14, 15, and 16) of the venturi to measure the local static pressure. The mixture exits from the venturi to the first stage cyclone (20) and a second stage cyclone (21). After that the separated air goes to the exit air tank (22), then goes through a gas-coal trap (23), which collects the remaining dust of coal from the exit air. Finally, the air goes out through the exit duct (25) and the solids particles are extracted to the secondary solid reservoir (26) to measure the solid flow rate. The solid is returned to the main solid reservoir which is controlled by a flow control valve 2 (28).
The details of the seven tested Venturi geometries, including the dimensions, in mm, are summarized in Table (1). However, the locations of the pressure taps, for each geometry, are shown in Fig. (2).

Table 1- Dimensions of the tested Venturis seven models.

Model No.(M)	$\beta = \dfrac{d_{th}}{D}$	Θ_1	Θ_2	D (mm)	d_{th} (mm)	L_1 (mm)	L_2 (mm)	L_3 (mm)	L_T (mm)	X_{th} (mm)	X_{max} (mm)
(1)	0.5	21°	8°	50.8	25.4	68.5	12.7	181.6	262.8	101.03	315.2
(2)	0.6	12°	10°	50.8	30.5	96.7	63.5	116.1	276.3	154.61	328.65
(3)	0.65	15°	4°	50.8	33	67.5	38.1	254.6	360.2	112.74	412.53
(4)	0.71	18°	6°	50.8	36.1	46.5	25.4	140.5	212.4	85.37	265.33
(5)	0.6	12°	10°	50.8	30.5	96.7	128.9	116.1	341.7	187.31	394.05
(6)	0.65	15°	4°	50.8	33	67.5	103.5	254.6	425.6	145.44	477.93
(7)	0.71	18°	6°	50.8	36.1	46.5	90.8	140.5	277.8	118.07	330.73
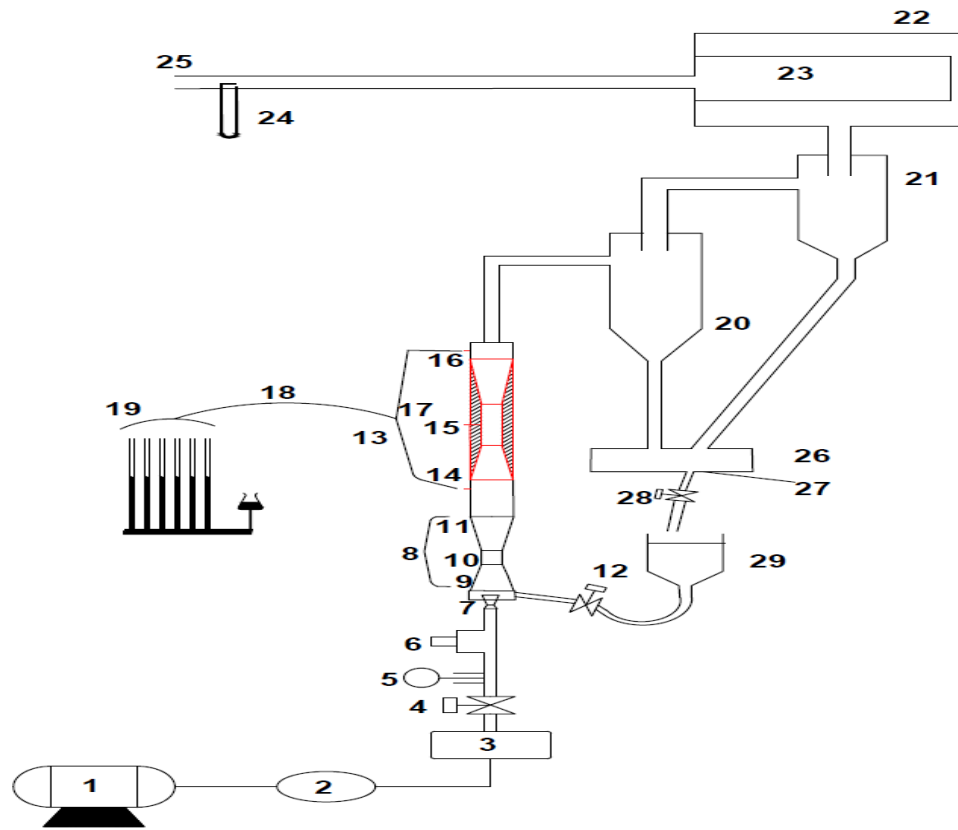
1 – Screw compressor, 2 – Air filter, 3 – Air tank, 4 – Pressure control valve, 5 – Orifice meter, 6 – Pressure regulator valve, 7 – Primary air convergent-divergent nozzle, 8 – Ejector, 9 – Constant pressure mixing section, 10 – Constant area mixing section, 11 – Diffuser section , 12 – Flow control valve, 13 – Venturi, 14 – Convergent section, 15 – Throat section, 16 – Divergent section, 17 – Pressure taps, 18 – Bundle of pressure hoses19–Multi U-tube manometers, 20 – First stage cyclone,21 – Second stage cyclone, 22 – Exit air tank, 23 – Air- Coal trap, 24 – Pitot static tube, 25 – Air exit, 26 – Secondary coal reservoir, 27 – Collected coal, 28 – Flow control valve, 29 – Main solid reservoir

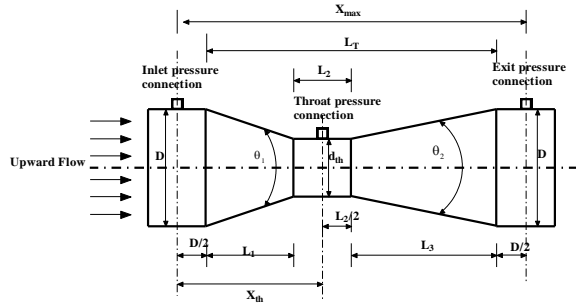Figure 1- Layout of the experimental setup

Figure 2- Geometrical parameters of Venturi models.

Seven airflow rates (0.0248, 0.02323, 0.024, 0.0248, 0.02323, 0.024 and 0.02323 kg/s) were investigated with solid to air mass loading ratios up to 8. The primary air stagnation pressure at the inlet is registered to be 8 bar and air temperature 300 K. The analysis of the uncertainty of the measurements is based on Kline and McClintock method [28]. The major sources of experimental uncertainty were discussed below. The gas flow rates were determined by an orifice flowmeter with an uncertainty of ±0.000755 kg/s. A weighing system was used to measure the mass of coal in a collected vessel with an uncertainty of ±0.1017 kg/s. A differential height of the manometer column was used to measure pressure drop along the venturi with an uncertainly of ±0.49 Pa and ±0.05 mm. The solid density was measured with an uncertainly of ±12 kg/m^3. The information regarding the measurement's accuracy is given in [29]. A mechanical sieving device is shown in Fig. (3) and a set of ASTM E11 standard sieves are used to separate a large quantity of coal to different particle size ranges.

Figure 3- A photograph of the mechanical sieving device

A sample from each quantity is sieved again but to sizes within the range of the quantity, collected and weighted. The cumulative particle size distribution is then determined for each size range and fitted accordingly to the Rosin-Rammler equation as in Ref. [30], which is given by:

$$Y_D = 1 - \exp(-(D_p/D_{p,m})^n) \tag{1}$$

where, YD is the mass fraction, is the mean particle diameter and n is the exponential coefficient. The mean diameter and the exponential coefficient, n which give the best fit are given in Table (2) for each size range. Figure (4) shows the measured size distribution combined with the best-fit equation.

Table 2- Coefficient of best fit to Eq. (1)

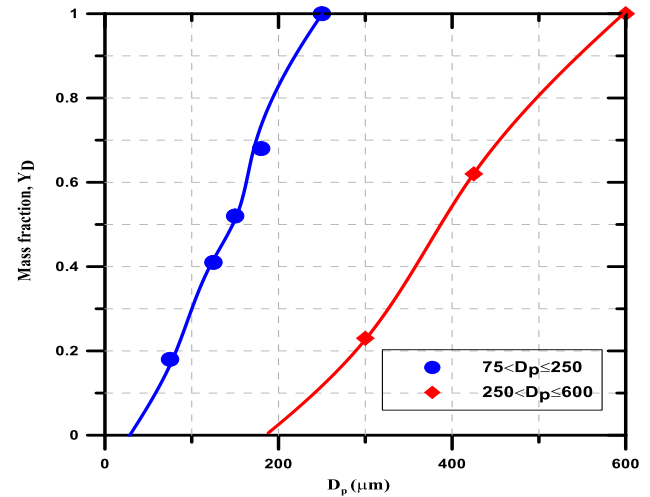| Size range (μm)	$D_{p,m}$ (μm)	n
<300	165	2.4
<600	430	3

Figure 4- Size distribution of coal particles

3. RESULTS AND DISCUSSION

Gas-Solid (air-coal) metering charts

As mentioned before and refer to Figs. (5 and 6), for pressure drop charts of seven models (M), as the loading ratio (Z) increases the pressure drop between the Venturi inlet and throat ΔP_{TP1} increases due to the gradual decrease in flow area. Also, for the diffuser pressure recovery in Fig. (6) as the loading ratio increases, the two-phase pressure recovery between the throat and Venturi exit ΔP_{TP2} increases. The figures illustrate that for every Stokes number defined

$$St. = \frac{\rho_p D_{p,m} U_g}{18\mu_g d_{th}} = \frac{2\dot{m}_g}{9\pi\mu_g d_{th}}(\frac{D_{p,m}}{D_{in}})^2 \frac{\rho_p}{\rho_g} \quad \text{and}$$

range from 3.75 to 37.49, the pressure drop ratio varies linearly with the loading ratio as previously found in Ref. [31].
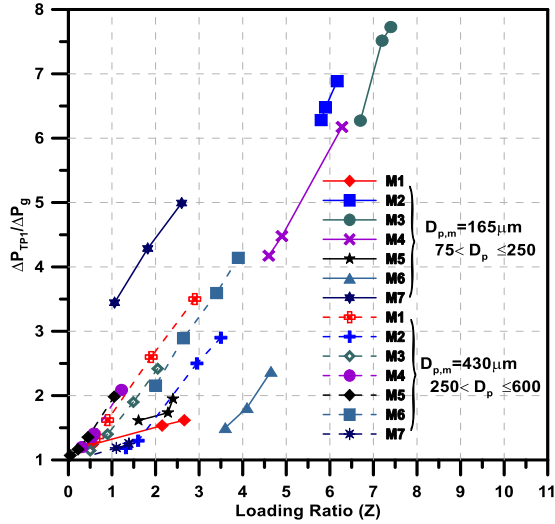
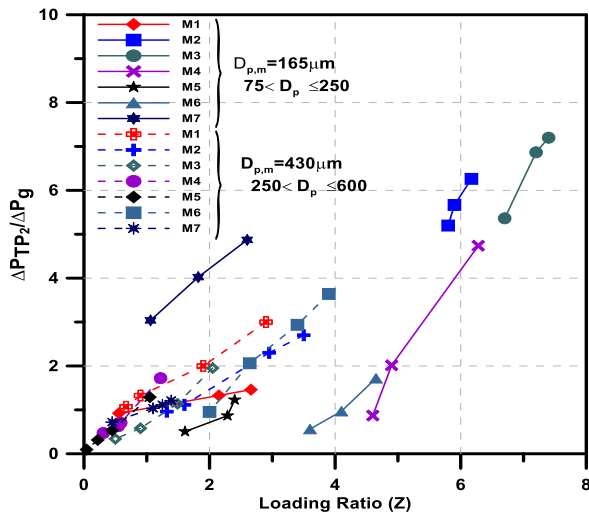Figure 5- Gas-Solid (air-coal) metering charts for air-coal pressure drop.

Figure 6- Gas-Solid (air-coal) metering charts for air-coal diffuser pressure recovery.

1.1 Effects of Stokes number

The effect of Stokes number on the pressure ratio is presented in Figs. (7 and 8) for the studied range of stokes number. for two different particle sizes, $D_{p,m} = 165\mu m$ and $D_{p,m} = 430\mu m$. From the figures, it is seen that the pressure ratio parameter, $(\Delta PTP/\Delta Pg-1)/Z$, for particle diameter $D_{p,m} = 165\mu m$ is smaller than that for particle diameter $D_{p,m} = 430\mu m$. This is because the loading ratio Z for particle diameter $D_{p,m} = 165\mu m$ is larger than that of particle diameter $D_{p,m} = 430\mu m$. Also, the range of Stokes number for

particle diameter $D_{p,m} = 165\mu m$ is smaller than particle diameter $D_{p,m} = 430\mu m$, because the particle diameter $D_{p,m}$ decreases for the same models that have the same throat diameter d_{th} and air velocity U_{air} for each model.
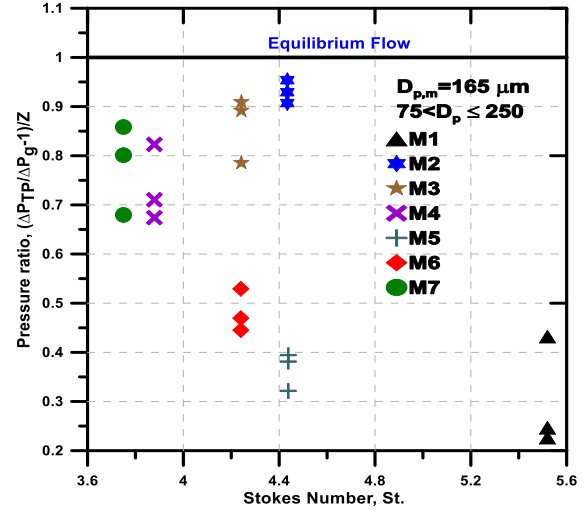

Figure 7- Effect of stokes number on the pressure ratio parameter for particle diameter (75<Dp≤250) for all tested models.
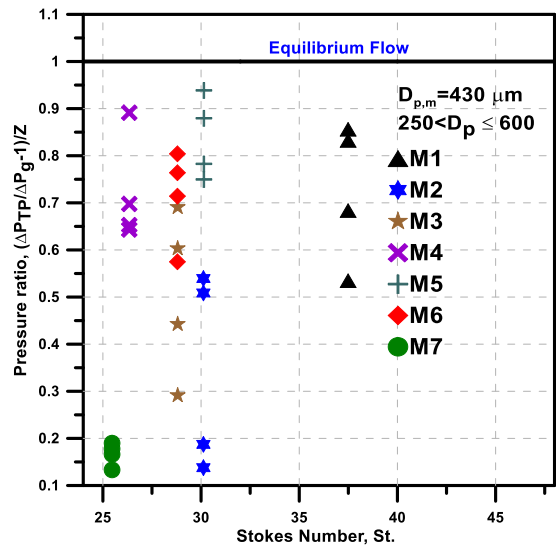

Figure 8- Effect of stokes number on the pressure ratio parameter for particle diameter (250<Dp≤600) for all tested models.

1.2 Venturi discharge coefficient (c_d)

For single-phase (air), the mass flow rate through Venturi can be calculated from

$$\dot{m} = \rho_f C_d W \frac{A_1}{\sqrt{(A_1/A_2)^2-1}} \sqrt{\frac{2g\rho_m \Delta h}{\rho_f}} \quad \text{for (Z=0)}$$

(2)

But, for two-phase (air – coal), the mass flow rate is computed from:

$$\dot{m}=\rho_{TP}Cd_{TP}W\frac{A_1}{\sqrt{(A_1/A_2)^2-1}}\sqrt{\frac{2g\rho_m\Delta h}{\rho_{TP}}}\quad\text{for }(0<Z\leq8)$$

(3)

From the previous charts and graphs of pressure drop through venturi included in Ref.[29], the two-phase correlation factor from the present experimental results can be obtained for all tested models. The experimental graphs illustrate the experimental correction factor and from the curve fitting, correlations for each model, and each particle diameters range are extracted. The error percent between the experimental correction factor and the correlated (reads from +1.1 to -1.15).

The discharge coefficient can also be obtained from the experimental results using equations (2 and 3). The correlation for the discharge coefficient factor can be then obtained from the curve fitting of the experimental discharge coefficient and loading ratio. The percentage error between the experimental discharge coefficient and that from correlation is then calculated. For all tested models, the values of the discharge coefficients, particle mass flow rates, loading ratios, Reynolds numbers, diameter ratios, convergent, throat, and divergent lengths and inlet and exit angles are tabulated as shown in Table (3). Generally, it is noticed that the increase of the loading ratio causes a clear reduction of the discharge coefficient. The results obtained from all models are presented in Fig. (9) with a linear representation of the measured to calculated discharge coefficients.
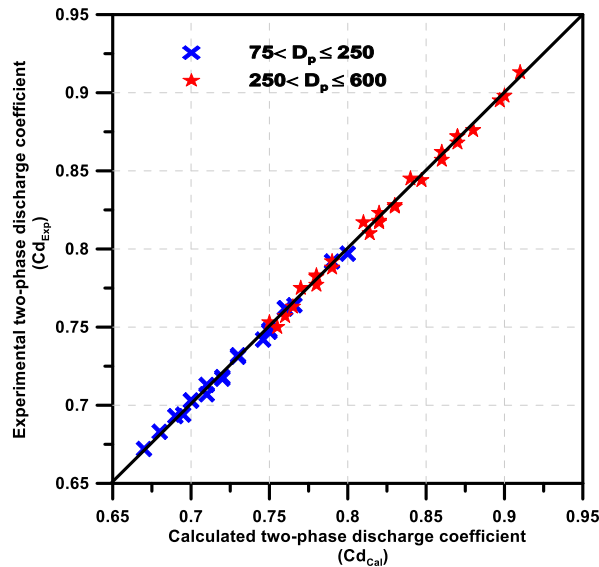

Figure 9- Calculated two-phase discharge coefficient to actual discharge coefficient for all tested models

Effect of Venturi throat length

The effect of Venturi throat length on the discharge coefficient is shown in Fig. (10) for air only and air-coal (250<Dp<=600 and 75<Dp<=250). As the throat length increases, the discharge coefficient decreases due to the increase in losses.
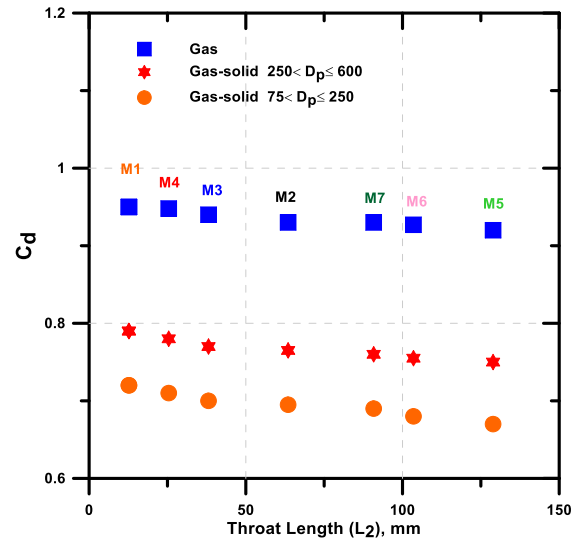

Figure 10- Effect of throat length on the discharge coefficient for all models.

Correction factor correlation

A new correlation for air – coal mass flow rate through Venturi, exploring the ranges of the studied geometrical parameters and particle sizes can be extracted from the experimental data. Correlation equation can be extracted from the curve fitting for the seven models for air – coal flow (Z>0) and can be written as:

$$Cd_{TP}=BZ+F\qquad\text{for}\quad 0<Z\leq8\qquad(4)$$

$$B=\frac{\theta_1^{6.9228}\times L_1^{4.6324}\times L_2^{0.9203}\times D_p^{0.68132}}{6.01879\times10^{17}\times\theta_2^{2.19873}\times L_3^{0.91091}}$$

(5)

$$F=\frac{5.29807\times10^{10}x\theta_2^{1.01325}\times L_3^{0.50213}}{\theta_1^{5.1645}\times L_1^{2.51034}\times L_2^{0.7986}\times D_p^{0.21345}}$$

(6)

where:

Cd_{TP} : the discharge coefficient of air -coal flow.

From the curve fitting, the error between the experimental and calculated two-phase correction factor can be obtained. A general correlation for the two-phase flow discharge coefficient to correction equation can be extracted for all studied tested models and particle size

Table (3): Two-phase flow discharge coefficient for all tested models

D_P	Model	C_{d1}	Z	St	Re_D	β	L_1	L_2	L_3	Θ_1	Θ_2	$\dot{m}_{P1}$
$75 < D_p \leq 250$	M1	0.72	2.66	5.52	150803.9	0.5	68.5	12.7	181.6	21°	8°	0.066
		0.76	2.15	5.52	150803.9	0.5	68.5	12.7	181.6	21°	8°	0.0533
		0.8	0.556	5.52	150803.9	0.5	68.5	12.7	181.6	21°	8°	0.0137
	M2	0.695	6.17	4.434	22455.47	0.6	96.7	63.5	116.1	12°	10°	0.1433
		0.73	5.9	4.434	22455.47	0.6	96.7	63.5	116.1	12°	10°	0.137
		0.766	5.8	4.434	22455.47	0.6	96.7	63.5	116.1	12°	10°	0.134
	M3	0.7	7.4	4.242	156307.7	0.65	67.5	38.1	254.6	15°	4°	0.1776
		0.73	7.2	4.242	156307.7	0.65	67.5	38.1	254.6	15°	4°	0.1752
		0.75	6.7	4.242	156307.7	0.65	67.5	38.1	254.6	15°	4°	0.1608
	M4	0.71	6.28	3.879	183551.5	0.71	46.5	25.4	140.5	18°	6°	0.156
		0.75	4.9	3.879	183551.5	0.71	46.5	25.4	140.5	18°	6°	0.1215
		0.79	4.6	3.879	183551.5	0.71	46.5	25.4	140.5	18°	6°	0.11408
	M5	0.67	2.4	4.438	91775.73	0.6	96.7	128.9	116.1	12°	10°	0.0557
		0.7	2.285	4.438	91775.73	0.6	96.7	128.9	116.1	12°	10°	0.053
		0.746	1.61	4.438	91775.73	0.6	96.7	128.9	116.1	12°	10°	0.037
	M6	0.68	4.65	4.24	166764.9	0.65	67.5	103.5	254.6	15°	4°	0.0624
		0.71	4.1	4.24	166764.9	0.65	67.5	103.5	254.6	15°	4°	0.0437
		0.76	3.6	4.24	166764.9	0.65	67.5	103.5	254.6	15°	4°	0.0254
	M7	0.69	2.6	3.75	171718.3	0.71	46.5	90.8	140.5	18°	6°	0.108
		0.72	1.82	3.75	171718.3	0.71	46.5	90.8	140.5	18°	6°	0.0952
		0.76	1.06	3.75	171718.3	0.71	46.5	90.8	140.5	18°	6°	0.0836
$250 < D_p \leq 600$	M1	0.79	2.9	37.489	150803.9	0.5	68.5	12.7	181.6	21°	8°	0.0719
		0.83	1.9	37.489	150803.9	0.5	68.5	12.7	181.6	21°	8°	0.047
		0.87	0.9	37.489	150803.9	0.5	68.5	12.7	181.6	21°	8°	0.02232
		0.91	0.67	37.489	150803.9	0.5	68.5	12.7	181.6	21°	8°	0.0166
	M2	0.765	3.5	30.1189	22455.47	0.6	96.7	63.5	116.1	12°	10°	0.0813
		0.79	2.95	30.1189	22455.47	0.6	96.7	63.5	116.1	12°	10°	0.06829
		0.83	1.6	30.1189	22455.47	0.6	96.7	63.5	116.1	12°	10°	0.03716
		0.87	1.32	30.1189	22455.47	0.6	96.7	63.5	116.1	12°	10°	0.03066
	M3	0.77	2.05	28.809	156307.7	0.65	67.5	38.1	254.6	15°	4°	0.049
		0.814	1.49	28.809	156307.7	0.65	67.5	38.1	254.6	15°	4°	0.035
		0.86	0.9	28.809	156307.7	0.65	67.5	38.1	254.6	15°	4°	0.0216
		0.897	0.5	28.809	156307.7	0.65	67.5	38.1	254.6	15°	4°	0.012
	M4	0.78	1.22	26.346	183551.5	0.71	46.5	25.4	140.5	18°	6°	0.0302
		0.82	0.586	26.346	183551.5	0.71	46.5	25.4	140.5	18°	6°	0.0145
		0.87	0.545	26.346	183551.5	0.71	46.5	25.4	140.5	18°	6°	0.0135
		0.9	0.31	26.346	183551.5	0.71	46.5	25.4	140.5	18°	6°	0.00768
	M5	0.75	1.05	30.144	91775.73	0.6	96.7	128.9	116.1	12°	10°	0.0244
		0.78	0.45	30.144	91775.73	0.6	96.7	128.9	116.1	12°	10°	0.0104
		0.82	0.22	30.144	91775.73	0.6	96.7	128.9	116.1	12°	10°	0.0051
		0.86	0.042	30.144	91775.73	0.6	96.7	128.9	116.1	12°	10°	0.00097
	M6	0.755	3.9	28.798	166764.9	0.65	67.5	103.5	254.6	15°	4°	0.0936
		0.81	3.4	28.798	166764.9	0.65	67.5	103.5	254.6	15°	4°	0.0816
		0.84	2.64	28.798	166764.9	0.65	67.5	103.5	254.6	15°	4°	0.06336
		0.88	2	28.798	166764.9	0.65	67.5	103.5	254.6	15°	4°	0.048
	M7	0.76	1.39	25.468	171718.3	0.71	46.5	90.8	140.5	18°	6°	0.0322
		0.78	1.25	25.468	171718.3	0.71	46.5	90.8	140.5	18°	6°	0.029
		0.82	1.1	25.468	171718.3	0.71	46.5	90.8	140.5	18°	6°	0.0255
		0.847	0.45	25.468	171718.3	0.71	46.5	90.8	140.5	18°	6°	0.01045

to have a comparison between experimental and correlated correction equation as shown in Figs. (11 to 12). The experimental results are compared with the predicted results in Figure (13) showing that the predicted values are a fair agreement with experimental results, with a relative deviation of less than +25% to -20% in all cases.
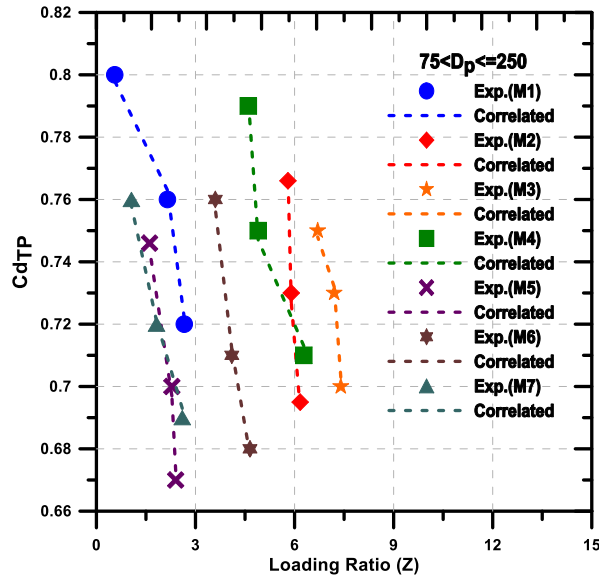

Figure 11- Correlated two-phase discharge coefficient to measured discharge coefficient for all models ($75<D_p≤250$).
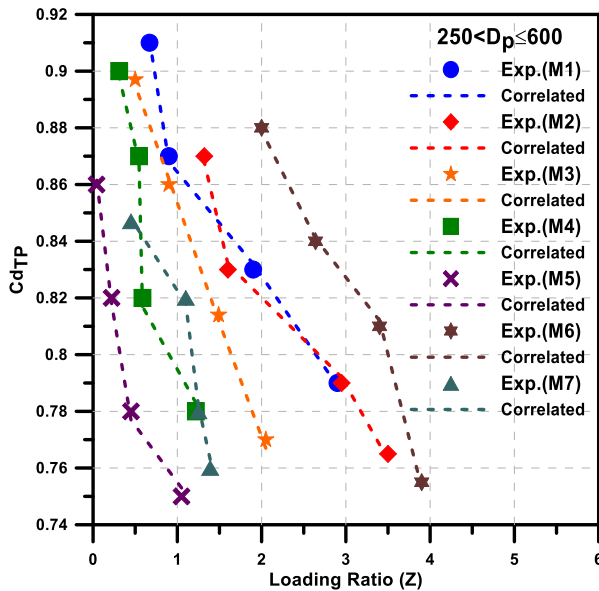

Figure 12-Correlated two-phase discharge coefficient to measured discharge coefficient for all models ($250<D_p≤600$)
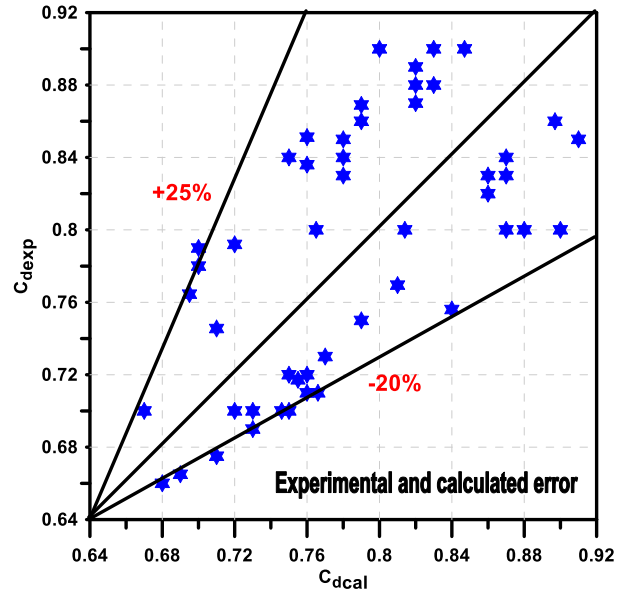

Figure 13- Experimental and calculated error from curve fitting.

1.3 Venturi loss coefficient (K_d)

The effect of the Venturi length effect on the loss coefficient is shown in Fig. (14) for air (gas) only and air (gas)-solid ($250<D_p≤600$ and $75<D_p≤250$).

$$K_d = \frac{(P_1 + \frac{\rho_f V_1^2}{2})-(P_2 + \frac{\rho_f V_2^2}{2})}{0.5\rho_f U_{in}^2} \tag{7}$$

As the throat length increases, the loss coefficient increases due to the increase of energy lost.

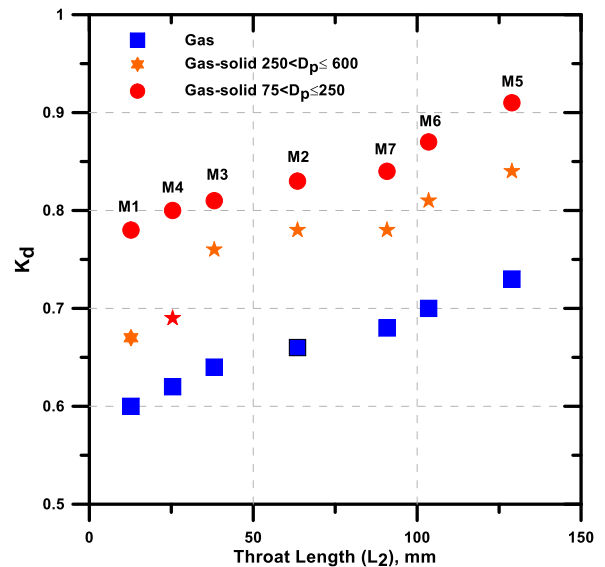
Figure 14- Throat length effect on loss coefficient for all models

4. CONCLUSIONS

In the present paper, gas-solid flow through a venturi is studied. The gas-solid venturi performance depends on two parameters. The first parameter is the operational condition (loading ratio Z, Stokes No. S_t., gas velocity U_g, and particle diameter D_p). The second is the geometrical venture parameters (inlet angle Θ_1, exit angle Θ_2, convergent length L_1, throat length L_2, divergent length L_3, and diameters ratio β). There is a pressure drop in the Venturi throat due to the gradual decrease in the flow area. The pressure at the Venturi exit is recovered due to the gradual increase in the flow area. As the loading ratio increases the pressure ratio increases and the pressure recovery increases. If the particle size decreases, the loading ratio increases, and the wall static pressure drop increases, the pressure ratio and total pressure ratio increase. As the throat length increases, the discharge coefficient decreases, and the loss coefficient increases. From the experimental results a new correlation for the two-phase flow discharge coefficient is deduced for the seven models studied in the present study and comparison between the experimental and calculated is done with error percentage ranges from +25% to -20%.

NOMENCLATURE

A_2	Venturi throat area (m^2)
D	Inlet/Exit diameter (mm)
D_p	Particle diameter (μm)
d	Venturi throat diameter (mm)
Δh	Reading of the manometer (pressure difference) (mm)
L1	Venturi convergent length (mm)
L2	Venturi throat length (mm)
L3	Venturi divergent length (mm)
LT	Venturi total length (mm)
ΔPg	Pressure drop between the venturi inlet and throat due to gas-only (Pa)
$\Delta PTTP$	Total pressure drop across the venturi due to particle-gas mixture (Pa)
ΔPTP	Pressure drop between the venturi inlet and throat due to particle-gas mixture (Pa)
$\Delta PTP/\Delta Pg$	Pressure drop ratio
$\Delta PTTP/\Delta PTP$	Total pressure drop ratio
$(\Delta PTP/\Delta Pg-1)/Z$	Pressure ratio parameter
St	Stoke number
U_g	Gas Velocity (m/s)
W	Expansion factor
X_{th}	Distance from the Venturi inlet to throat pressure taps
Xmax	Distance from the Venturi inlet to outlet pressure taps
Z	Solids loading ratio ($\dot{m}p/\dot{m}g$)
ρ_g	Gas density (kg/m^3)
ρ_m	Manometer fluid density, (kg/m^3)
ρ_p	Solid density (kg/m^3)
ρ_{TP}	Two-phase flow density (kg/m^3)
β	Diameters ratio (d/D)
Θ_1	Venturi inlet angle, degree
Θ_2	Venturi exit angle, degree

6. REFERENCES

[1] Allen R.W.K. and van Santen A., "Designing for pressure drop in Venturi scrubbers: the importance of dry pressure drop", Chemical Engineering, 61, pp.203-211,1996.

[2] Allen R.W.K., "Prediction of Venturi scrubber grade efficiency curves using the contacting power law", Powder Technology, 86, pp.137-144, 1996.

[3] Giddings D., Azzopardi B.J., Aroussi A. and Pickering S.J., "Optical investigation of a long-throated Venturi conveying inert spherical particulate with size range similar to pulverized coal", Powder Technology, 207, pp.370-377, 2011.

[4] Zhansong W. and Fei X., "Optimization of Venturi tube design for pipeline pulverized coal flow measurements", Energy Power, 2, pp.369-373, 2008.

[5] Cai L., Jiawei H., Hengyu L., Liu S., Gaoyang Y., Xiaoping C., and Changsui Z., "Resistance characteristics of pressure letdown in dense-phase pneumatic conveying", Chemical Engineering, 49, pp.511-518, 2016.

[6] Kai L., Haifeng L., Xiaolei G., Xiaolin S., Shunlong T., and Xin G., "Experimental study on flow characteristics and pressure drop of gas–coal mixture through venturi", Powder Technology, 268, pp.401- 411, 2014.

[7] Azzopardi B.J., Teixeira S.F.C.F. and Pulford C.I., "A quasi-one-dimensional model for gas-solid flow in ventures", Powder Technology, 102, pp.281-288, 1999.

[8] Haifeng L., Xiaolei G., Wanjie H., Kai L., and Xin G., "Flow characteristics and pressure drop across the Laval nozzle in dense phase pneumatic conveying of the pulverized coal", Chemical Engineering and Processing, 50, pp.702-708, 2011.

[9] Cai L., John R., Liu S., Gaoyang Y., Xiaoping C., and Changsui Z., "Experimental investigation of pressure letdown flow characteristics in dense-phase pneumatic conveying at high pressure", Powder Technology, 277, pp.171-180, 2015.

[10] Haifeng L., Xiaolei G., Peng L., Kai L., and Xin G., "Design optimization of a venturi tube geometry in dense-phase pneumatic conveying of pulverized coal for entrained-flow gasification", Chemical Engineering, 120, pp.208-217, 2017.

[11] Richard H., "System for measuring entrained solid flow", New York, N.Y., Babcock and Wilcox Technology Inc, 1980.

[12] Herbreteau C. and Board R., "Experimental study of parameters which influence the energy minimum in horizontal gas-solid conveying", Powder Technology, 112, pp.213–220, 2000.

[13] Reader-H., Brunton W.C., Gibson J.J., Hodges D., and Nicholson I.G., "Discharge coefficients of Venturi tubes with standard and non-standard convergent angles", Flow Measurement and Instrumentation, 12, pp.135-145, 2001.

[14] Gary O. and Anthony P., "Flow-Rate measurement in two-phase flow", Fluid Mech., 36, pp.149-172, 2004.

[15] Wang Z.L., Ding Y.L. and Ghadiri M., "Flow of a gas-solid two-phase mixture through a packed bed", Chemical and Particle Science, 59, pp. 3071-3079, 2004.

[16] Hu H.L., Xu T.M., Hui S.E. and Zhou Q.L., "A novel capacitive system for the concentration measurement of pneumatically conveyed pulverized fuel at power stations", Flow Measurement and Instrumentation, 17, pp.87-92, 2006.

[17] Ali M., Qi Y. C. and Mehboob K., "A Review of Performance of a Venturi Scrubber", Nuclear Science and Technology, 4(19), pp.3811-3818,2012.

[18] Ying X., Qiang Z., Tao Z. and Xili B., "An overreading model for nonstandard Venturi meters based on H correction factor", Flow Measurement, 61, pp.100-106, 2015.

[19] Grazia M., Mario De S. and Bruno P., "Two-phase flow measurements at high void fraction by a Venturi Meter", Flow Measurement, 77, pp.167-175,2014.

[20] Schade K.P., Erdmann H.J., Hadrich Th., Schneider H., Frank T. and Bernert K., "Experimental and numerical investigation of particle erosion caused by pulverized fuel in channels and pipework of coal-fired power plant", Powder Technology 125, pp.242-250, 2002.

[21] Xiaoqiang Z., Dongfeng Z., Wang and Yide G., "Transportation characteristics of gas-solid two-phase flow in a long-distance pipeline", Particuology, 21, pp.196-202,2015.

[22] Thiago F. de P., Rodrigo B. and José T. F., "Gas-Solid Flow Behavior in a Pneumatic Conveying System for Drying Applications: Coarse Particles Feeding with a Venturi Device", Chemical Engineering, 5, pp.225-238, 2015.

[23] Richard H. B., "Particle Collection and Pressure Drop in Venturi Scrubbers", Chemical Engineering, 12, pp.40-50,1973.

[24] Giddings D., Azzopardi B.J., Aroussi A. and Pickering S.J., "Absolute measurement of pneumatically conveyed powder using a single long throat venturi", Powder Technology, 172, pp.149-156,2007.

[25] El-Behery S. M., El-Askary W. A., Ibrahim K. A. and Mofreh H. Hamed., " Porous Particles Drying in a Vertical Upward Pneumatic Conveying Dryer ", International Journal of Aerospace and Mechanical Engineering, pp.110-125,2011.

[26] El-Askary W. A., Ibrahim K. A., El-Behery S. M., Mofreh H. Hamed. and Al-Agha M.S.," Performance of vertical diffusers carrying gas-solid flow: experimental and numerical studies", Powder Technology, 273, pp.19-32,2015.

[27] Zhang J., Xiao L., Zhaoyang C., Yu Z., Gang L., Kefeng Y. and Tao L., "Gas-Lifting Characteristics of Methane-Water Mixture and Its Potential Application for Self-Eruption Production of Marine Natural Gas Hydrates". Energies, 240, pp.1-22, 2018.

[28] Holman J.P., "Experimental methods for engineers", 7th ed. McGraw-Hill,2000.

[29] Ghonim, T. A., Sheha, M., Sakr, I. M. and El-Askary, W. A., " Experimental study on Gas-Solid mixture flows in a Venturi", 18th International Conference on Applied Mechanics and Mechanical Engineering, 3-5 April, pp.18-29,2018.

[30] El-Behery S. M., El-Askary W. A., Ibrahim K. A. and Mofreh H. Hamed., "Numerical and experimental studies of heat transfer in particle-laden gas flows through a vertical riser", International Journal of Heat and Fluid Flow, 30, pp.118-130,2012.

[31] Doss, E.," Analysis and application of solid-gas flow inside a venturi with particle interaction", International Journal of Multiphase Flow, Vol. I 1, No. 4, pp. 445-458,1985.